Chapter 4

LASER DIODE MODEL AND COMPUTATIONAL TECHNIQUES

4.1 Simulation

Simulation offers a powerful tool if it is used creatively and appropriately. Computer models can provide an enormous amount of insight into how physical systems work. The optimum simulation is one which captures the right physical process, and does so using a method which reflects the reality. The power of simulation is due to the fact that it permits us to set up a method of solution simply and in a form that we can easily understand, even in situations which are physically very complex and difficult. Setting up the solution scheme gives us considerable insight into the mathematics which describes the problem. This can reflect the physical reality and it shows us graphically how the mathematics capture the physical situation. Once the equations have been solved, we begin the process of looking at the graphical output in detail and using simple intuitive models to try to understand it. This is essential if we are to be confident the results are right and it is a powerful way of gaining insight into many aspects of the system. Studying the results shows how those inputs control the response of the system being studied.

In this chapter, the simulation result of the 980 nm InGaAs/GaAs strained quantum well material system is presented, using the theory described in Chapter

2 and Chapter 3. The required 980 nm lasing wavelength is well within the range of achievable wavelengths using the strained InGaAs/GaAs structures. However, only a few lasers emitting at 980 nm and designed for pumping Er^{3+} doped fibre amplifiers have been reported. There is also a lack of data on reliability and degradation characteristics at the power densities required although encouraging results have recently been reported at lower power densities.

In view of this, when designing high-performance laser diodes, a detail understanding of the optical properties of semiconductor heterostructure is very essential. It is still difficult to find an adequate approach to their description that would be appropriate for device modeling. It is common practice to use heavily empirical approaches fitted to experimental data in a narrow range. In this simulation, a physics-based approach to modeling the optical properties of quantum well semiconductor laser has been developed and implemented.

4.2 980 nm Laser Diode Model

Every simulation starts by designing the model structure. In view of the immense potential and growing importance of 980nm quantum well lasers, it is an essential task to explore their material properties theoretically in order to design the quantum well laser structures. One of the laser structure that lasing at 980 nm is $In_xGa_{1-x}As$ material system which is employed for a pumping source for erbium-doped optical fiber amplifier. The structural design of this type of typical multiple-quantum-well (MQW) laser diode is presented and adopted as the

simulation model in this chapter. The typical MQW structure includes the quantum wells, a cladding layer, and a cap layer.

Figure 4.1 illustrates the schematic structure of a **$In_{0.2}Ga_{0.8}As/GaAs$** QW laser diode. This physical model is a layered structure with finite thickness layers sandwiched between semi-infinite substrate and cap layer. As in a real life epitaxial growth, building the structure proceeds from substrate (bottom layer) to cap layer (top layer). Table 4.1 tabulates the compositions and layer thickness of the structure. The design of this QW laser structure is to obtain the emission wavelength of 980 nm. There are three quantum wells in the quantum well layer. The well width is 70 Å and barrier width is 150 Å and the corresponding compressive strain imposed is 2.29% as computed using equation (3.5.1).

This semiconductor laser diode is a forward bias *p-i-n* junction as illustrated in Figure 2.1. Free carriers (electron and holes) are injected into the active region (i) by forward biasing the laser diode. In this QW strained laser diode, the active region is the strained QW layer which consists of three quantum wells.

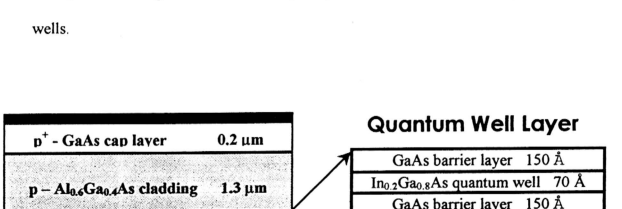

*Figure 4.1 Schematic structure of **$In_{0.2}Ga_{0.8}As/GaAs$** 980 nm QW laser diode*

Layer	*Thickness*	*Doping Concentration*
p^+ - GaAs cap layer	0.2 μm	1×10^{19} cm^{-3}
n – $Al_{0.6}Ga_{0.4}As$ cladding	1.3 μm	5×10^{17} cm^{-3}
GaAs barrier layer	150 Å	Nominally undoped
$In_{0.2}Ga_{0.8}As$ quantum well	70 Å	Nominally undoped
GaAs barrier layer	150 Å	Nominally undoped
$In_{0.2}Ga_{0.8}As$ quantum well	70 Å	Nominally undoped
GaAs barrier layer	150 Å	Nominally undoped
$In_{0.2}Ga_{0.8}As$ quantum well	70 Å	Nominally undoped
GaAs barrier layer	150 Å	Nominally undoped
n – $Al_{0.6}Ga_{0.4}As$ cladding	1.3 μm	5×10^{17} cm^{-3}
n^+ - GaAs substrate	0.2 μm	3×10^{18} cm^{-3}

Table 4.1 Compositions and layer thickness of *$In_{0.2}Ga_{0.8}As/GaAs/GaAs$ 980 nm QW* structure

4.3 Computational Techniques

The process of modeling consists of three principle stages:

(a) designing the modeled structure

(b) scheduling the simulations

(c) computing the properties of this structure according to the theories in Chapter 2 and Chapter 3 using *HS_Design Semiconductor Heterostructure Modeling Software*, Version 1.0.

4.3.1 Simulation Conditions

Before running the simulation, the simulation conditions need to be specified. Two parameters are global to the modeled structure. These are the ambient temperature, T_o and residual doping concentration, N_o. The ambient temperature is set to be 300 K corresponds to the real ambient environment. The residual doping concentration is very difficult to be controlled in a real life. It reflects the practical capabilities of the common epitaxial growth technologies, such as MBE and MOCVD. The residual doping concentration is assumed to be the same for wells and barriers in the QW layer. In this simulation, it is set to be $1\times10^{15}cm^{-3}$ which catches the practical needs.

4.3.2 Model Computations

The process of simulation is implemented following the general theories described in Chapter 2 for bulk structure and Chapter 3 for quantum well structure.

In the first step, the electronic properties of the structure are calculated at given carrier concentration and temperature. The band structure is obtained using equations (2.5.2) and (2.5.3). Then the calculation of the distribution over the energy bands is performed using equations (2.5.5).....(2.5.10).

In the second step, the optical properties of the structure are computed on the basis of already known electronic properties. The complex permittivity is computed using equations (2.2.1) and (2.2.2) at given photon energy, carrier concentration and temperature.

The electronic properties and optical properties are obtained accordingly as described below.

(A) Band Structure

The computations of band structure are based on the scheme in section 2.5 of Theoretical Background. All the bands and valleys in the conduction band are considered isotropic and all the valence bands are parabolic. The non-parabolicity of the conduction is taken into consideration by equation (3.5.2).

(B) Quantum Subband Structure

Section 3.6 of Quantum Well Lasers explains the quantum subband structure. The conduction and valence bands are considered to be parabolic. The spectra of bound state electrons and holes are approximated by a parabolic dispersion law in equation (3.5.6).

(C) QW Band Edge Profile

The QW layer is assumed to be electrically neutral as a whole. However, it is not locally neutral. The injected carrier charge imbalance in the wells bends the QW band edges and the calculation of the self-consistent electrostatic potential is required as described in section 3.6.1 by equation (3.6.7).

(D) Interband Transitions

The optical transitions between the valence and conduction bands give contribution to gain in the spectral range above the band gap as formulated in section 2.5.2 of Theoretical Background. From equation (2.5.20), the Coulomb interaction between the electron and hole modifies their states thus excitonic transitions occur below the band gap. Band gap shrinkage due to the exchange-correlation interaction is included using equation (2.5.25). The dynamic

polarization of free carrier plasma is incorporated using equation (2.5.26) and the anomalous dispersion is also taken into account by equation (2.5.27).

(E) Intraband Transitions

The general formulation of the intraband transition contribution to the imaginary part of permittivity is given in section 2.5.3 of Theoretical Background by using equation (2.5.19).

(F) Spectral Broadening

Due to the intraband scattering, the electron and holes states are not stationary and hence their energies are not certain. The related uncertainty in this energy together with the finite coherence time of the states result in broadening of the spectral line. This spectral broadening is incorporated by using equation (2.4.2) as a delta-function.

After the computations of the electronic properties and optical properties of the model have been performed, the purpose is to obtain the real part and the imaginary part of permittivity by using equations (2.2.2) and (2.5.28) respectively. Then the index of refraction and extinction coefficient are found by using equations (2.2.6) and (2.2.7) as described in section 2.2 of Theoretical Background. Subsequently, by applying TMM explained in section 2.3, the optical characteristics of the entire model structure, such as optical field distribution and propagation constant can be solved.